ELSEVIER

Middle Miocene–early Pliocene paleo-oceanic environment of Japan Sea deduced from geochemical features of sedimentary rocks

S. Kimura[a], N. Shikazono[b,*], H. Kashiwagi[b], M. Nohara[c]

[a]*Quintessa Japan Limited, Queens Town A7-707 Minatomirai, Yokohama, 220-6007, Japan*
[b]*Department of Applied Chemistry, Faculty of Science and Technology, Keio University, 3-14-1, Hiyoshi, Kohoku, Yokohama 223-8522, Japan*
[c]*Geological Survey of Japan, 1-1-1, Higashi, Tsukuba, Ibaraki 305-8567, Japan*

Abstract

Chemical and isotopic compositions (Sr isotopic ratio, major elements, trace elements, rare earth elements, total carbon, nitrogen, and sulfur contents) of rock samples collected from middle Miocene to early Pliocene sedimentary rocks on the Oga Peninsula, northern Japan, were analyzed to elucidate the paleo-oceanic environment of the Japan Sea. The rocks studied were shales from the Nishikurosawa, Onnagawa and Funakawa formations in stratigraphically ascending order. The Onnagawa sedimentary rocks in the lower (ca. 12.6–11.4 Ma), middle (ca. 10.6–9.0 Ma) and upper (ca. 8.3–7.0 Ma) horizons have high Mo/Al, Ni/Al, and Ba/Al ratios and high total organic carbon as well as high K/Ti and $^{87}Sr/^{86}Sr$ ratios and a positive Eu anomaly. These geochemical variations imply high primary productivity, and reducing conditions indicative of a deep paleo-ocean. The formation of petroleum source rocks on these horizons is attributed to increasing of nutrient delivery from the terrigenous system, which may have been induced by strong wind from Asian continent related to the uplift of Himalayan and Tibetan regions.
© 2003 Elsevier B.V. All rights reserved.

Keywords: Paleo-oceanic environment; Miocene; Japan Sea; Rare earth elements; Strontium isotope; Geochemistry; Sediment chemistry

1. Introduction

Highly siliceous sedimentary rocks of Miocene age are widely distributed in the Circum-Pacific region including Japan (Iijima, 1994), California (Ingle, 1981), Kamchatka (Bazhenova and Arefiev, 1990), and Sakhalin (Ivanov and Shcherban, 1983). These rocks, known as hard shale, have been the subject of extensive geological investigation in the exploration for fossil-fuel resources (oil and natural gas). The Miocene sedimentary rocks on the Oga Peninsula, northern Japan, have been the focus of many stratigraphic, paleontological and structural studies because this region hosts an almost complete record of successive sedimentations. Previous studies of this region established the standard Tertiary stratigraphic succession of Japan. The Tertiary stratigraphy of the Peninsula is regarded as a type locality of the Miocene green tuff belt of northern Japan, and is characterized by a thick sequence of more than 1000 m of marine volcanic and sedimentary rocks, with intense hydrothermal and diagenetic alteration.

* Corresponding author. Tel.: +81-45-566-1567; fax: +81-45-566-1551.

E-mail address: sikazono@applc.keio.ac.jp (N. Shikazono).

Complementing these geological studies, the change in the paleo-oceanic environment of the Japan Sea during the Miocene has been investigated by a number of authors (e.g., Tada, 1991; Watanabe et al., 1994; Yamamoto and Watanabe, 1994). Watanabe et al. (1994) and Yamamoto and Watanabe (1994) obtained bulk compositional data for sedimentary rocks from several localities in an attempt to elucidate the depositional environment of the Onnagawa siliceous organic-rich deposits. However, no systematic
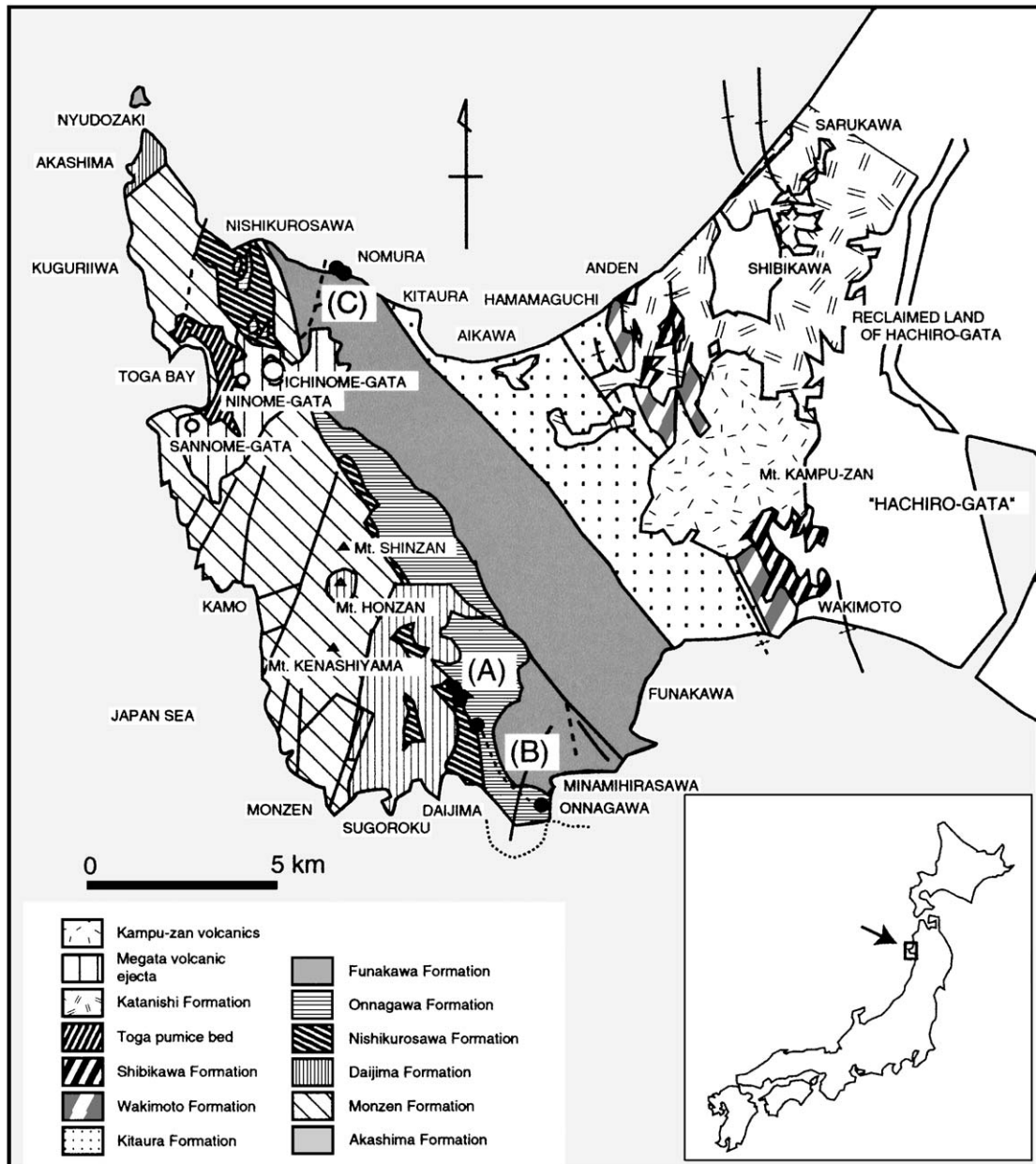

Fig. 1. Geologic map of the Oga Peninsula, northeast Japan (modified after Huzioka and Takayasu, 1965). (A) Daijima route (Nishikurosawa Formation), (B) Onnagawa route (Onnagawa Formation), (C) Nomura route (Funakawa Formation).

geochemical study has been carried out for a comprehensive sequence of sedimentary rocks from the early to late Miocene to the early Pliocene.

The Kuroko ore deposit, a volcanogenic massive sulfide-sulfate deposit in Japan, has been reported to have been formed by hydrothermal venting from the seafloor, related to an extensional environment in the Japan Sea in the middle Miocene (14–16 Ma; Shikazono, 1988). The formation of the Kuroko deposits indicates that the Japan Sea at the Nishikurosawa stage was host to intense hydrothermal activity, which continued after the middle Miocene to form the Kuroko deposit. Utada et al. (1982) suggested based on studies of the hydrothermal alteration that this
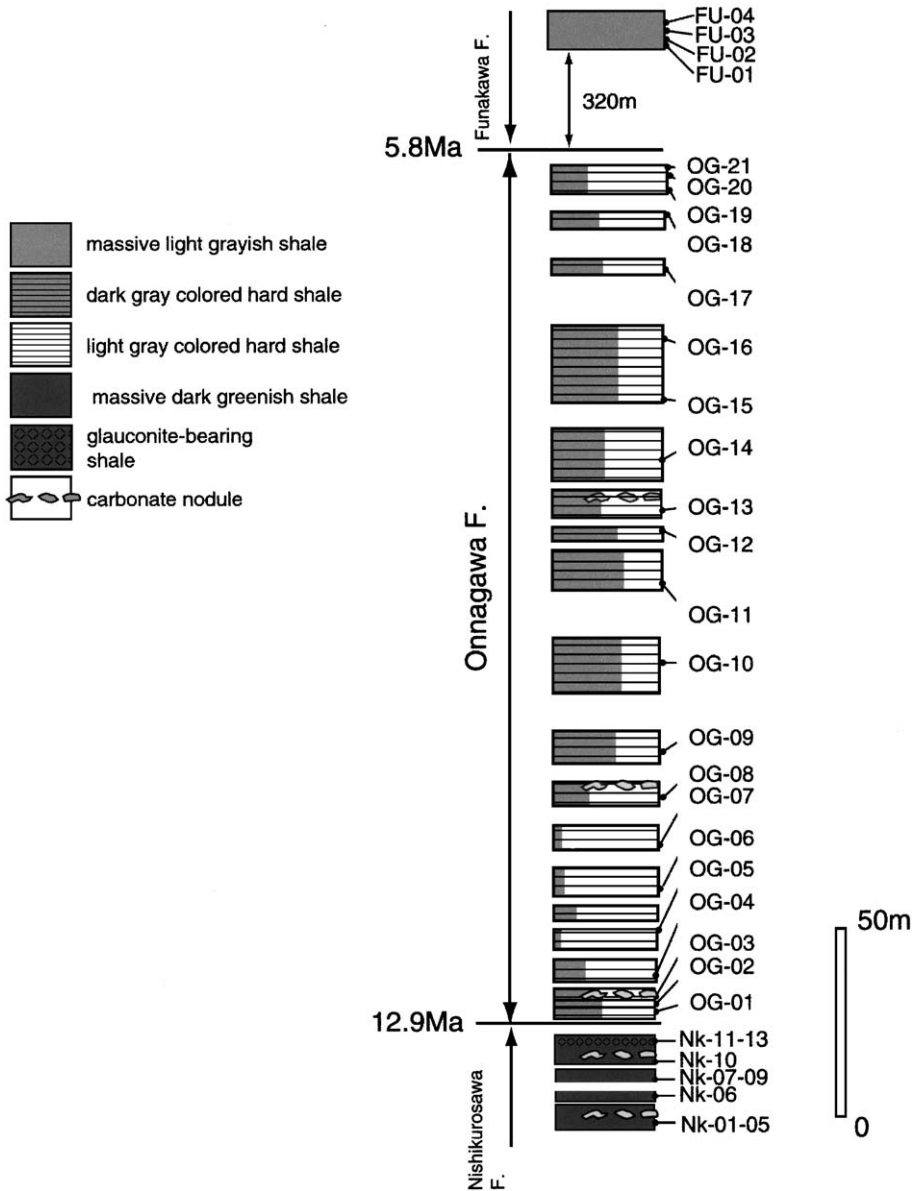

Fig. 2. Schematic stratigraphic and lithologic section of the study area. Numbers indicate sampling points. Age data are from Koizumi and Matoba (1991).

hydrothermal activity continued from the end of the Nishikurosawa to late in the Onnagawa stage, although the activity decreased in the Kuroko mining area, northern Honshu, Japan. It is possible that this hydrothermal activity influenced the geochemistry of sedimentary rocks. However, this possibility has yet to be examined.

The objective of the present study was to deduce the paleo-oceanic environmental change during the mid-late Miocene into the early Pliocene based on systematic geochemical data obtained for middle Miocene–early Pliocene sedimentary rocks (12.9 to 5.8 Ma) from the Oga Peninsula, northern Japan. The causes of the observed geochemical variations are discussed with respect to implications for biogenic productivity, bottom water redox condition, and climate change in relation to the tectonics of the Asian continent.

2. Geologic setting and sample descriptions

The study area was located in the west of the Oga Peninsula, northern Honshu Island, Japan (Fig. 1). The area is composed mostly of Miocene–Pliocene sedimentary rocks. Rocks of the Nishikurosawa, Onnagawa and Funakawa Formations were examined (Fig. 1).

The Nishikurosawa Formation, 180 m in thickness, is mainly composed of siltstone, mudstone, conglomerate and sandstone. The tuffaceous sandstone contains *Miogypsina* and *Operculina* fossils, while the siltsimes and mudstones contain foraminiferal fossils such as *G. birnageal*, and *G. denseconnexa*, indicating Zone N.9 by Blow (1969). The upper part of the formation is characterized by glauconite-bearing sedimentary rock. The 300-m-thick Onnagawa Formation, conformably overlying the Nishikurosawa Formation, is dominantly composed of siliceous shale (hardshale) and shale. The hardshale is a well-known potential rock for petroleum exploration (e.g. Taguchi, 1961). The sedimentary rocks are characterized by organic-rich laminated diatomaceous deposits, siliceous microfossils, fish scales and fish bones, but very poor in foraminiferal fossils. The Onnagawa Formation is estimated to have deposited from 12.9 to 5.8 Ma based on diatoms (Koizumi and Matoba, 1991). The Onnagawa Formation is unconformably underlain by the Funakawa Formation, with thickness of about 1000 m. The Funakawa Formation is composed of siltstone with intercalated tuff and tuffaceous siltstone and occasional foraminiferal fossils and siliceous microfossils.

A total of 38 samples were collected from three routes, Daijimazawa, Onnagawa and Nomura routes (13, 21 and 4 samples from the Nishikurosawa, Onnagawa and Funakawa Formations, respectively).

The samples from the Nishikurosawa Formation on the Daijimazawa route are massive shale containing small amounts of carbonate nodules and glauconite. The samples from the Onnagawa Formation are dark-colored hardshale rarely containing rare carbonate nodule. The samples from the Funakawa Formation on the Nomura route are light-colored massive shale, with very rare carbonate.

The stratigraphic horizons of the 38 samples are shown in the columnar section (Fig. 2).

3. Analytical procedure and results

3.1. X-ray diffraction analysis and optical microscopy

The minerals were identified by X-ray diffraction (XRD) analysis and observation under optical microscope.

The analytical results are given in Table 1, and typical XRD patterns for the Nishikurosawa, Onnagawa and Funakawa sedimentary rocks are shown in Fig. 3.

The major minerals in the Nishikurosawa Formation are quartz, feldspar, pyrite, dolomite and smectite. Quartz is round in shape with grains of 20–40 μm in size, suggesting a detrital origin. The grain size of the feldspar and smectite is generally $10-30$ μm, but rarely up to 1 mm for feldspar. Relics of

Table 1
Mineralogy of the sedimentary rocks studied

Lithology	Formation	Mineralogy
Shale	Funakawa	Qz, Fd, Sm, Ill, Ch, Py
Hard shale	Onnagawa	Qz, Fd, Ill, Sm, Ch Py
Shale	Nishikurosawa	Qz, Fd, Do, Sm, Py

Qz: quartz, Fd: feldspar, Sm: smectite, Ill: illite, Ch: chlorite, Py: pyrite, Do: dolomite.
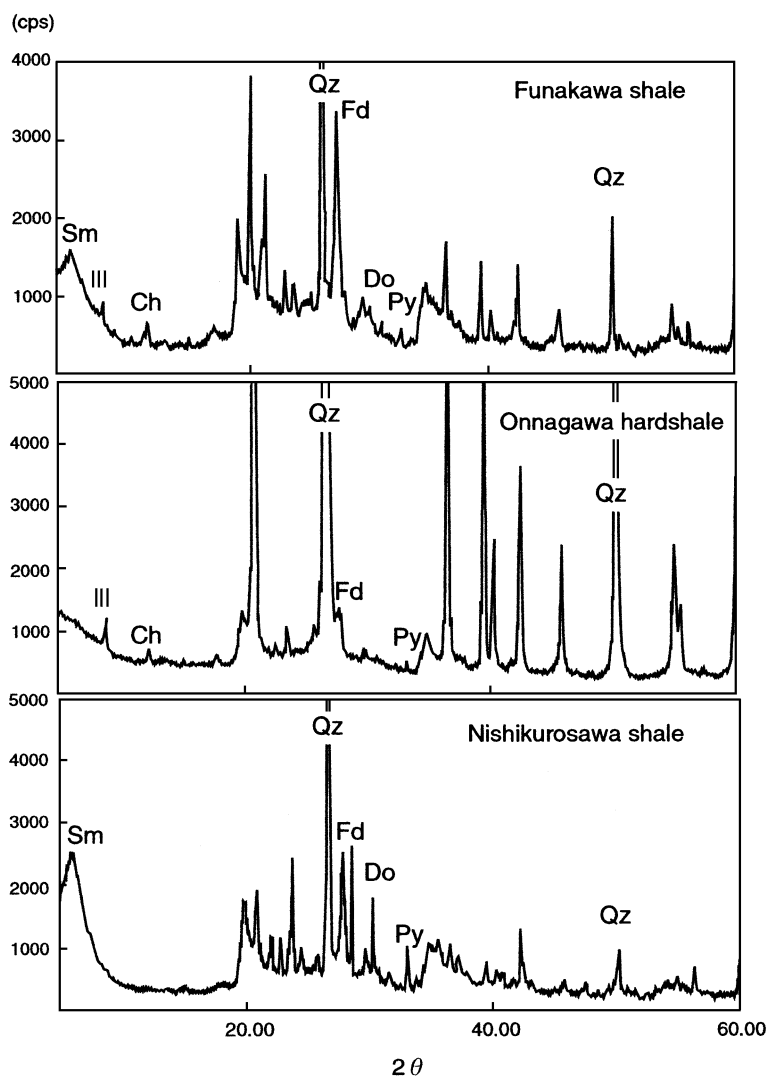
Fig. 3. X-ray diffraction pattern of representative samples studied. (A) Funakawa shale (Sample No. FK-04), (B) Onnagawa hard shale (Sample No. OG-8), and (C) Nishikurosawa shale (Sample No. NK-07).

foraminiferal fossils are filled with carbonate with a grain size of more than 100 μm. Euhedral pyrite of 5–20 μm are also present. Quartz is dominant in the Onnagawa sedimentary rocks and is microcrystalline (<5 μm) and round in shape, suggesting a diatomaceous origin. Accessory minerals include pyrite, feldspar, illite, chlorite and smectite. Most pyrite larger than 100 μm is framboidal. Microcrystalline feldspar and clay minerals are less than 2 μm in diameter. The interstitial matrix consists of dolomite and organic matter.

The major minerals of the Funakawa shale are quartz, feldspar, pyrite, illite, smectite and chlorite. Detrital quartz is 10–40 μm in size, while feldspar, illite, smectite and chlorite are 2–30 μm in diameter. Rare relicts of diatoms (siliceous shells) can also be found.

The abundance of quartz is distinctly different in each formation. Quartz is very abundant in the Onnagawa Formation but not in the Funakawa and Nishikurosawa Formations, the later containing abundant carbonate of foraminiferal fossil origin.

Table 2
Major elements, N, S, and C contents of sedimentary rocks studied

Sample No.	Daizima-sawa area													Onnagawa-sawa area				
	NK-01	NK-02	NK-03	NK-04	NK-05	NK-06	NK-07	NK-08	NK-09	NK-10	NK-11	NK-12	NK-13	OG-01	OG-02	OG-03	OG-04	OG-05
Lithology	sh	sh	sh	sh	sh	sh	sh	sh	sh	sh	sh	sh	sh	h. sh	h. sh	h. sh	h. sh	h. sh
Color	dk. gn.	dk. gn.	dk. gn.	dk. gn.	dk. gn.	dk. gn.	dk. gn.	dk. gn.	dk. gn.	dk. gn.	dk. gn.	dk. gn.	dk. gn.	dk. and lgt. gr.	dk. and lgt. gr.	dk. and lgt. gr.	dk. and lgt. gr.	dk. and lgt. gr.
SiO_2 (wt.%)	59.11	57.49	57.95	58.87	58.94	57.53	57.56	56.39	53.01	56.47	56.21	59.83	60.58	86.79	80.38	83.48	89.50	91.44
TiO_2	0.95	0.96	0.90	0.89	0.90	0.92	0.89	0.95	0.91	0.96	0.92	0.89	0.90	0.16	0.28	0.19	0.12	0.12
Al_2O_3	15.7	16.4	15.4	15.5	16.5	17.3	16.5	16.5	16.2	16.8	17.0	16.5	16.6	4.5	6.9	4.8	2.6	3.1
Fe_2O_3*	7.76	7.85	7.99	7.89	7.70	7.74	7.98	7.35	7.92	8.36	9.63	7.72	7.62	1.29	2.95	1.98	1.14	0.95
MnO	0.037	0.037	0.037	0.031	0.015	0.012	0.041	0.067	0.172	0.031	0.017	0.015	0.017	0.007	0.017	0.025	0.015	0.010
MgO	4.14	4.45	4.44	4.38	4.03	4.11	3.84	4.34	4.89	4.39	4.05	3.87	3.87	0.59	1.10	0.59	0.25	0.39
CaO	2.16	2.47	1.92	2.04	2.55	3.14	3.84	4.56	6.59	3.71	3.22	2.45	2.54	0.23	0.36	0.42	0.27	0.28
Na_2O	0.76	0.80	0.40	0.50	1.05	1.29	1.36	1.25	1.28	1.30	1.52	1.05	1.08	0.14	0.25	0.14	0.07	0.06
K_2O	1.22	1.28	1.21	1.27	1.69	1.70	1.62	1.71	1.74	1.46	1.97	1.67	1.67	0.68	1.17	0.92	0.51	0.52
P_2O_5	0.105	0.125	0.084	0.093	0.108	0.083	0.112	0.127	0.262	0.152	0.116	0.089	0.089	0.013	0.062	0.125	0.058	0.080
LOI	8.09	8.15	9.63	8.48	6.51	6.16	6.29	6.76	7.06	6.36	5.34	5.96	5.00	5.65	6.52	7.36	5.47	3.08
TN (wt.%)	0.23	0.22	0.05	0.05	0.03	0.03	0.03	0.03	0.03	n.a.	0.03	0.03	0.03	0.12	0.16	0.18	0.14	0.09
TS	3.05	2.72	2.71	2.77	1.65	2.02	2.83	1.88	1.22	n.a.	1.26	1.33	1.14	0.95	1.73	1.52	1.07	0.14
TOC	0.71	0.64	0.77	0.78	0.50	0.34	0.43	0.40	0.32	n.a.	0.29	0.40	0.41	2.49	2.46	3.60	2.74	1.46
Carbonate carbon	0.06	0.05	0.12	0.08		0.02	0.23	0.53	1.07	n.a.	0.03	0.02	0.01	0.02	0.07	0.08	0.07	0.04
TOC/TN	3.12	2.99	15.54	17.18	15.17	12.29	12.58	12.67	11.11	n.a.	10.63	13.75	14.75	20.41	15.62	20.44	19.93	16.95

dk. gn.; dark greenish, lgh gr; light grayish, sh; shale, h. sh; hard shale, n.a.; not analysed. No entry below detection limit.

																Nomura area			
OG-06 h. sh dk. and lgt. gr.	OG-07 h. sh dk. and lgt. gr.	OG-08 h. sh dk. and lgt. gr.	OG-09 h. sh dk. and lgt. gr.	OG-10 h. sh dk. and lgt. gr.	OG-11 h. sh dk. and lgt. gr.	OG-12 h. sh dk. and lgt. gr.	OG-13 h. sh dk. and lgt. gr.	OG-14 h. sh dk. and lgt. gr.	OG-15 h. sh dk. and lgt. gr.	OG-16 h. sh dk. and lgt. gr.	OG-17 h. sh dk. and lgt. gr.	OG-18 h. sh dk. and lgt. gr.	OG-19 h. sh dk. and lgt. gr.	OG-20 h. sh dk. and lgt. gr.	OG-21 h. sh dk. and lgt. gr.	FK-01 sh lgt. gr.	FK-02 sh lgt. gr.	FK-03 sh lgt. gr.	FK-04 sh lgt. gr.
80.98	79.96	86.99	84.98	77.25	80.48	91.96	81.19	85.60	84.19	86.77	85.34	86.09	83.93	82.88	80.61	67.43	69.40	67.44	65.71
0.25	0.30	0.20	0.21	0.32	0.21	0.11	0.32	0.22	0.23	0.20	0.19	0.20	0.23	0.24	0.32	0.55	0.54	0.61	0.59
7.1	7.3	5.0	5.7	9.5	5.6	3.0	7.2	5.7	8.0	4.9	4.8	5.5	6.1	7.6	8.6	14.6	13.9	15.5	15.5
2.23	2.90	1.73	1.45	2.21	3.12	0.89	1.79	2.53	0.82	0.86	2.29	1.22	1.88	1.95	2.19	4.96	4.38	4.20	5.22
0.016	0.030			0.020	0.029		0.004	0.033			0.015	0.005	0.009	0.076	0.014	0.063	0.068	0.037	0.057
1.21	1.16	0.60	0.58	1.31	0.62	0.35	0.83	0.81	0.85	0.51	0.60	0.74	0.75	1.04	1.02	2.20	1.97	1.98	2.45
0.52	0.55	0.14	0.17	0.38	0.33	0.28	0.28	0.37	0.20	0.16	0.39	0.32	0.14	0.36	0.38	2.01	1.69	1.22	1.18
0.18	0.25	0.02	0.08	0.11	0.15	0.01	0.14	0.11	0.07		0.11	0.08	0.13	0.14	0.34	1.16	1.42	1.19	1.22
1.18	1.33	0.89	1.05	1.33	1.22	0.48	1.58	1.05	1.13	0.93	1.02	0.99	1.18	1.11	1.49	2.02	2.10	2.08	2.28
0.043	0.081	0.030	0.430	0.684	0.413	0.053	0.041	0.044	0.020	0.312	0.059	0.020	0.024	0.024	0.037	0.084	0.070	0.068	0.080
6.29	6.14	4.43	5.35	6.92	7.85	2.90	6.62	3.51	4.47	5.38	5.50	4.83	5.58	4.61	5.03	4.90	4.43	7.29	5.68
0.14	0.13	0.11	0.13	0.14	0.19	0.06	0.19	0.08	0.09	0.13	0.13	0.11	0.13	0.09	0.12	0.08	0.09	0.09	0.53
1.45	1.89	0.14	0.20	1.63	1.47	0.09	0.96	0.08	0.11	0.19	0.70	0.84	1.01	0.07	0.98	0.69	0.74	0.44	0.49
2.44	2.12	1.76	2.42	2.45	4.09	1.22	3.38	1.17	1.60	2.69	2.87	2.10	2.32	1.06	1.66	0.60	0.71	0.76	0.87
0.06	0.05	0.05	0.14	0.20	0.04		0.02	0.02					0.07	0.25		0.25	0.12		0.09
17.24	15.79	16.47	18.73	17.41	22.01	19.91	17.65	15.47	18.41	21.30	22.31	19.97	17.89	11.62	14.36	7.09	7.76	8.76	1.62

Pyrite is abundant in the Nishikurosawa Formation, but decreases in abundance in the Onnagawa and Funakawa Formations.

Clay minerals also differ, with the Nishikurosawa Formation being characterized by smectite, the Onnagawa Formation containing an illite + chlorite assemblage, and the Funakawa Formation having smectite + illite + chlorite.

3.2. Organic carbon, carbonate carbon, sulfur and nitrogen contents

Total carbon, sulfur and nitrogen were analyzed using an automatic element analyzer (NA2500, CE Instrument) in NCS mode. The results are given in Table 2. The analytical uncertainty was ± 3% for total carbon (TC), total organic carbon (TOC), and total sulfur (TS).

The organic carbon content is higher in the Onnagawa hard shale (av. 2.29 wt.%) than in the Nishikurosawa (av. 0.50) and the Funakawa (av. 0.73) shales.

Shales from the Onnagawa Formation also have ratios of TOC/N which range up to high values than those of Nishikurosawa and Funakawa shales.

Average carbonate carbon content of the Nishikurosawa, Onnagawa and Funakawa is 0.18 ± 0.31, 0.06 ± 0.07, 0.12 ± 0.10 wt.%, respectively. The higher carbonate carbon content from Nishikurosawa Formation probably relates to greater occurrences of relics of foraminiferal fossils in the shales than in the Onnagawa and Funakawa shales.

Average TS content of the Nishikurosawa, Onnagawa and Funakawa is 2.05, 0.82, and 0.59 wt.%, respectively.

3.3. Major element contents

Major element contents were analyzed by X-ray fluorescence spectroscopy (XRF) according to the method of Irino (1997). The analytical uncertainties were better than 2.0%.

The data are listed in Table 2, and the average analytical data are compared with Post-Archean Australian Shale (PAAS; Taylor and McLennan, 1985) in Fig. 4.

The average elemental compositions of the Nishikurosawa shale are similar to the PAAS (including SiO_2 and Al_2O_3), except for higher $Fe_2O_3^*$, MgO

and CaO contents, and lower MnO and K_2O content.

In contrast, the average SiO_2 content of the Onnagawa Formation is much higher (89.12 wt.%), while the major elements are lower.

The average major element contents of the Funakawa Formation are similar to the PAAS, with slightly lower TiO_2, Al_2O_3, $Fe_2O_3^*$, MnO, K_2O and slightly higher contents of all other elements.

3.4. Minor element and rare earth element contents

Minor element and rare earth element (REE) contents were analyzed by inductively coupled plasma mass spectroscopy (ICP-MS) according to method of Imai (1990). The analytical uncertainty was ± 2%. The minor element data are given in Table 3 and are compared with the PAAS (Taylor and McLennan, 1985) in Fig. 5.

The Zn (av. 1160 ppm) contents of the Nishikurosawa Formations are very high, while all other elements occur are at the same level as the PAAS.

The average contents of minor elements of the Onnagawa Formation are mostly lower than those of the Nishikurosawa Formation and typically less than half the abundance given for the PAAS. However, the Cu, Zn, Mo, Ba and U contents anomalously high compared to the PAAS. The average minor element contents of the Funakawa Formation are lower than the PAAS.

The average contents of minor element contents of the Funakawa Formation are lower than the PAAS, due to the slightly higher SiO_2 content of the Funakawa Formation.

The REE data are given in Table 4. The REE patterns of the Nishikurosawa, Onnagawa and Funakawa shales normalized against the NASC REE content (Goldstein and Jacobsen, 1988) are shown in Fig. 6.

The Eu anomaly (Eu/Eu*), Ce anomaly (Ce/Ce*) and La/Yb ratio were calculated using the following equations.

$$Eu/Eu* = (2Eu/Eu_{NASC})/(Sm/Sm_{NASC} + Gd/Gd_{NASC})$$

$$Ce/Ce* = (3Ce/Ce_{NASC})/(2La/La_{NASC} + Nd/Nd_{NASC})$$

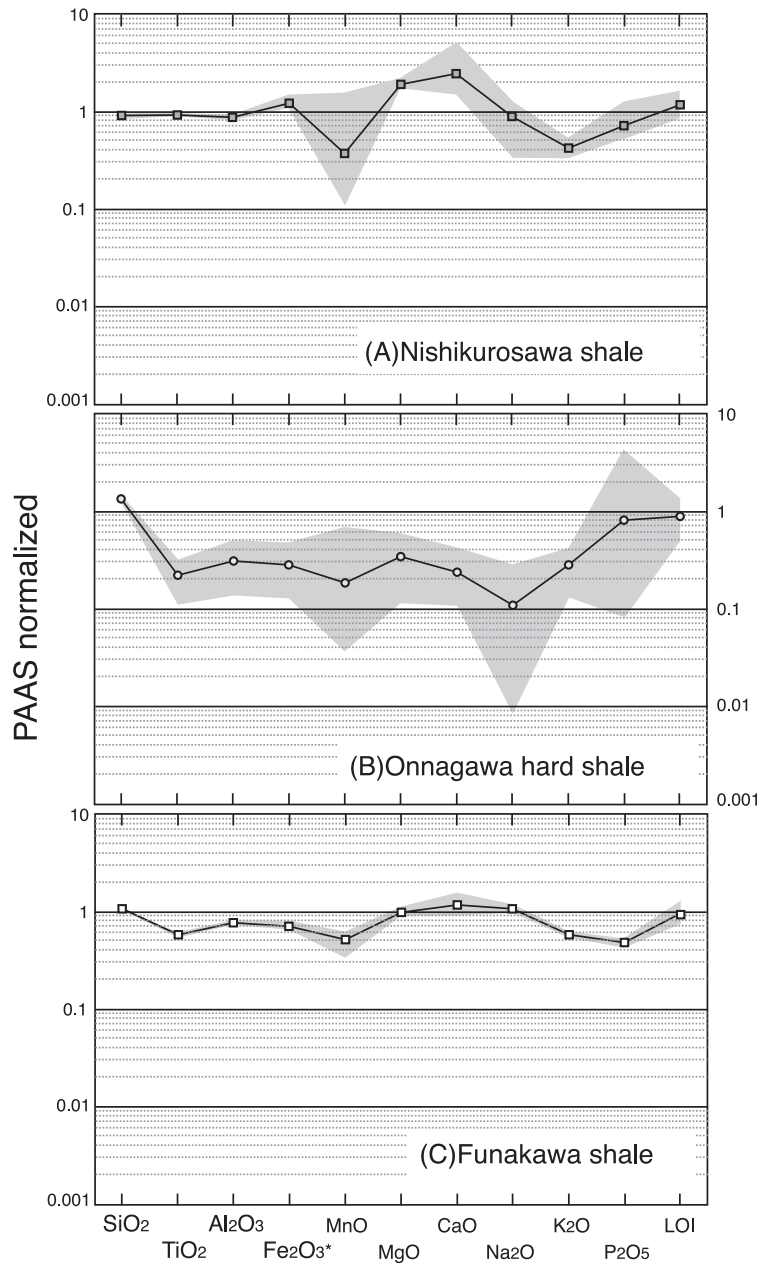$$La/Yb = (La/La_{NASC})/(Yb/Yb_{NASC})$$

Fig. 4. Average abundance of major elements of sedimentary rocks relative to the PAAS by Taylor and McLennan (1985). (A) Nishikurosawa shale, (B) Onnagawa hard shale, (C) Funakawa shale.

The REE pattern of the Nishikurosawa shale exhibits a slight light REE enrichment (La/Yb; 0.55 ± 0.09) and plots close to the line of the NASC normalized value = 1. A positive Ce anomaly (Ce/Ce*; 1.13 ± 0.08) and positive Eu anomaly (Eu/Eu*;

1.27 ± 0.06) were also identified in the Nishikurosawa Formation.

The REE patterns of the Onnagawa shale are plotted within $0.1-1$ of the NASC normalized value. The Ce and Eu anomalies are variable,

Table 3
Minor elements contents of sedimentary rocks studied

	Daizima-sawa area													Onnagawa-sawa area				
Sample No.	NK-01	NK-02	NK-03	NK-04	NK-05	NK-06	NK-07	NK-08	NK-09	NK-10	NK-11	NK-12	NK-13	OG-01	OG-02	OG-03	OG-04	OG-05
Lithology	sh	sh	sh	sh	sh	sh	sh	sh	sh	sh	sh	sh	sh	h. sh	h. sh	h. sh	h. sh	h. sh
Color	dk. gn.	dk. gn.	dk. gn.	dk. gn.	dk. gn.	dk. gn.	dk. gn.	dk. gn.	dk. gn.	dk. gn.	dk. gn.	dk. gn.	dk. gn.	dk. and lgt. gr.	dk. and lgt. gr.	dk. and lgt. gr.	dk. and lgt. gr.	dk. and lgt. gr.
Sc (ppm)	17.59	21.18	17.05	16.99	18.71	14.73	16.44	17.13	18.30	16.40	14.97	15.70	17.81	3.36	5.98	1.59	1.86	2.63
V	107.69	139.26	106.55	99.04	90.02	98.49	103.34	127.51	120.61	120.22	98.52	99.13	108.60	59.07	58.84	99.16	87.13	43.04
Cr	41.69	50.99	52.33	52.86	42.24	42.65	55.11	69.88	53.46	57.27	49.83	62.25	37.15	24.86	32.87	35.43	24.70	17.63
Co	14.32	18.53	17.05	14.39	17.66	15.12	17.76	18.91	21.54	20.54	15.45	15.63	14.98	7.40	15.32	11.15	12.54	7.95
Ni	27.34	27.58	39.15	29.86	30.01	20.87	25.00	25.98	28.33	31.54	19.25	62.70	19.52	35.00	44.86	48.11	45.69	10.15
Cu	20.11	23.70	25.76	22.96	18.28	13.99	17.39	20.59	19.03	19.65	11.86	15.94	15.62	53.86	59.12	55.31	36.79	25.38
Zn	99.22	380.90	165.73	334.02	295.59	97.39	279.95	90.40	87.89	97.22	72.68	12956.47	131.23	138.36	166.43	94.98	81.50	19.11
Rb	35.74	37.17	37.74	40.34	48.62	36.96	36.70	34.03	30.92	33.73	52.94	47.66	48.57	23.46	40.95	23.08	16.95	18.26
Sr	142.07	175.00	124.58	138.24	202.27	273.91	295.44	308.90	364.64	235.72	266.45	210.90	238.29	30.33	38.25	22.11	27.33	28.33
Y	32.21	37.40	27.31	27.68	31.24	19.77	17.54	22.16	46.52	29.62	22.75	22.95	23.25	3.05	8.65	4.53	4.95	8.18
Zr	161.71	172.23	165.94	171.11	176.23	151.77	125.96	123.19	115.30	120.54	123.09	152.24	154.08	35.28	60.52	42.50	23.10	29.96
Nb	8.33	8.39	9.14	8.76	8.71	8.32	8.10	6.68	6.52	6.79	7.65	8.06	8.50	2.40	3.65	2.89	1.68	2.87
Mo	10.83	12.11	12.22	9.23	4.75	1.29	2.81	1.39	0.91	4.38	0.85	1.85	1.31	10.38	14.20	22.18	17.67	4.96
Ba	208.87	389.88	225.84	249.95	864.36	1391.72	1692.49	2469.89	2390.52	796.79	859.20	841.16	601.75	1504.61	1169.25	1346.12	1375.12	1281.03
Hf	3.53	3.40	3.67	3.82	3.56	3.29	2.86	2.88	2.47	2.69	2.90	3.21	3.41	0.81	1.37	0.95	0.55	0.64
Ta	0.57	0.51	0.56	0.56	0.55	0.57	0.52	0.48	0.43	0.45	0.51	0.53	0.55	0.21	0.36	0.23	0.12	0.17
Th	3.07	3.06	3.05	3.53	3.55	3.44	3.30	2.87	2.65	2.57	2.86	3.08	3.35	2.70	4.18	1.91	1.76	2.07
U	3.28	2.70	3.39	3.23	3.04	1.52	1.18	1.68	1.45	1.48	1.02	1.71	1.47	3.59	7.62	3.31	4.77	4.63

Abbreviations are the same as those in Table 2. No entry below detection limit.

|																Nomura area			
OG-06 h. sh dk. and lgt. gr.	OG-07 h. sh dk. and lgt. gr.	OG-08 h. sh dk. and lgt. gr.	OG-09 h. sh dk. and lgt. gr.	OG-10 h. sh dk. and lgt. gr.	OG-11 h. sh dk. and lgt. gr.	OG-12 h. sh dk. and lgt. gr.	OG-13 h. sh dk. and lgt. gr.	OG-14 h. sh dk. and lgt. gr.	OG-15 h. sh dk. and lgt. gr.	OG-16 h. sh dk. and lgt. gr.	OG-17 h. sh dk. and lgt. gr.	OG-18 h. sh dk. and lgt. gr.	OG-19 h. sh dk. and lgt. gr.	OG-20 h. sh dk. and lgt. gr.	OG-21 h. sh dk. and lgt. gr.	FK-01 sh lgt. gr.	FK-02 sh lgt. gr.	FK-03 sh lgt. gr.	FK-04 sh lgt. gr.
6.69	5.43	3.73	3.54	8.58	4.31	1.51	6.18	4.09	4.76	3.71	3.18	3.63	5.13	4.39	4.86	7.07	5.84	7.29	6.72
48.44	53.29	61.37	182.26	46.59	13.16	13.18	24.30	26.35	35.89	68.02	64.75	40.57	35.73	30.86	33.38	55.69	47.32	55.72	59.00
31.08	27.94	24.06	37.08	38.36	39.64	14.43	34.25	23.34	24.59	26.87	29.22	22.11	25.19	19.27	27.47	21.10	20.93	19.77	22.32
15.54	20.34	2.24	1.55	13.32	10.95	1.17	10.04	12.34	2.61	1.01	11.21	7.92	8.57	21.94	11.58	7.01	6.80	4.58	6.60
43.87	55.82	7.07	17.16	44.45	64.65	10.03	29.77	15.11	12.07	6.72	32.33	28.29	31.44	19.43	30.92	15.55	36.43	12.70	13.68
56.44	56.71	30.38	64.40	108.91	60.25	23.11	252.69	35.78	45.05	29.32	50.25	79.35	125.12	23.53	94.11	16.50	12.53	15.84	16.00
20.90	265.58	45.13	83.19	186.23	641.62	54.28	32.26	71.28	51.33	6.39	86.18	108.31	134.40	55.59	177.18	82.65	79.76	58.34	59.64
37.73	39.06	30.33	32.72	37.95	39.14	16.42	47.02	31.91	30.99	26.39	29.39	24.02	31.62	31.85	38.78	52.43	47.66	44.21	55.03
42.32	37.20	18.81	22.14	29.92	38.13	18.80	29.39	25.98	21.30	15.24	27.56	21.22	26.68	33.04	35.86	107.38	93.89	79.56	79.72
10.75	12.15	4.86	5.30	11.69	17.97	5.41	7.69	8.38	27.46	9.55	6.18	7.56	8.79	9.57	7.34	14.71	14.41	18.07	17.44
48.31	57.33	44.40	41.96	55.69	41.23	20.44	59.95	42.99	43.21	33.26	38.08	35.48	42.37	43.50	56.96	73.06	60.65	72.66	75.92
3.76	3.41	3.18	3.12	3.97	3.07	1.90	4.49	2.80	3.11	2.49	2.61	2.52	3.53	2.99	4.47	5.57	5.31	5.82	6.00
7.17	8.96	8.48	20.71	11.21	19.02	4.63	15.38	4.82	2.67	8.27	14.78	10.77	12.33	6.67	7.89	2.47	1.96	1.89	0.90
997.36	1180.32	1045.05	1022.74	1683.73	6769.83	2297.28	2118.78	1591.49	1294.31	838.98	1634.39	951.26	1022.86	1056.85	2072.42	654.31	638.16	688.37	742.34
1.32	1.50	1.00	1.03	1.53	0.97	0.60	1.61	1.17	1.22	0.88	0.97	1.10	1.27	1.27	1.70	2.70	2.33	2.76	2.72
0.36	0.33	0.25	0.32	0.36	0.30	0.12	0.44	0.26	0.32	0.24	0.24	0.27	0.32	0.35	0.45	0.66	0.66	0.67	0.69
3.81	3.36	2.73	3.58	4.55	4.06	1.87	5.99	3.66	3.89	6.72	3.59	3.33	3.92	4.19	3.62	6.73	6.59	6.45	7.19
4.22	4.92	4.86	9.06	21.05	13.00	1.67	7.28	4.05	4.01	3.75	7.35	9.05	5.46	4.55	4.99	1.91	2.06	3.11	3.22
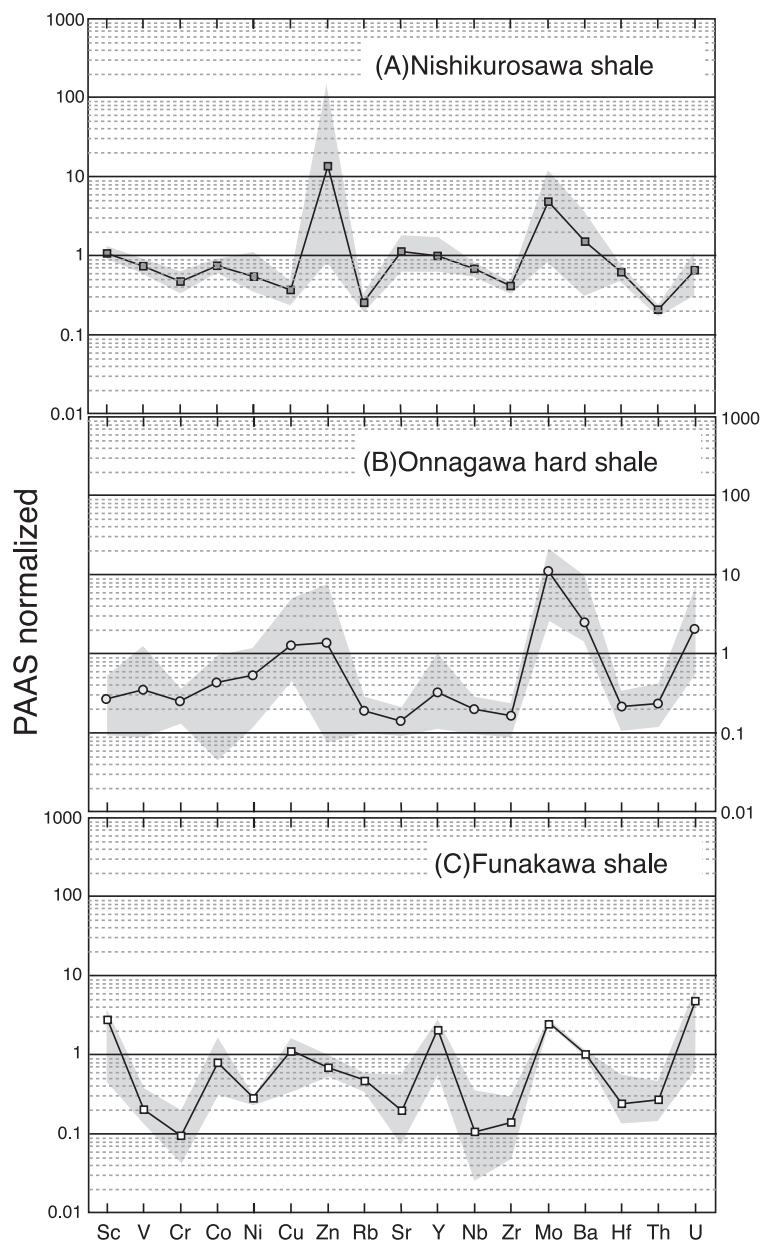
Fig. 5. Average abundance of minor elements of sedimentary rocks relative to the PAAS by Taylor and McLennan (1985). (A) Nishikurosawa shale, (B) Onnagawa hard shale, (C) Funakawa shale.

and the La/Yb ratio of the Onnagawa shale is 0.56 ± 0.14.

The Funakawa Formation exhibits a weak Eu and Ce anomaly (Eu/Eu*; 1.09 ± 0.05, Ce/Ce*; 1.20 ± 0.01).

3.5. Sr isotopic ratio

The $^{87}Sr/^{86}Sr$ ratio of bulk rock samples was analyzed using a Finnigan MAT-262 mass spectrometer. The analytical uncertainty was 0.000011.

The data are shown in Table 5 and Fig. 7. The $^{87}Sr/^{86}Sr$ ratios of the Onnagawa Formation are higher (av. 0.710851) than those of the Nishikurosawa Formation (av. 0.706237) and the Funakawa Formation (av. 0.708068).

4. Discussion

The influences of terrigenous components, biogenic productivity and hydrothermal activity on the chemical and isotopic compositions of sedimentary rocks are considered below based on the above geochemical and mineralogical data.

A correlation coefficients between the content of analyzed elements relative to Al_2O_3 are shown in Table 6.

4.1. Terrigenous components

Fig. 8 shows that the TiO_2, Sc, Nb, Hf, and Zr contents positively correlate to Al_2O_3 content. Al_2O_3, TiO_2, Sc, Nb, Hf and Zr are thought to be largely of terrigenous origin (e.g. Murray et al., 1991).

The relationship between Al_2O_3 and TiO_2 differs markedly between the Nishikurosawa and Funakawa Formations. The terrigenous components of the Nishikurosawa are relatively rich in TiO_2 compared with the Onnagawa and Funakawa Formations.

The $^{87}Sr/^{86}Sr$ ratios are consistent with the Al_2O_3 and TiO_2 data. The average $^{87}Sr/^{86}Sr$ ratio of the Nishikurosawa is 0.706237 which is similar to that of the average andesitic (island arc) rock region, while the Onnagawa (0.710851), and Funakawa (0.708068) samples are plotted in the region of average acidic rocks.

The acidic rock component has two possible sources; continental or island-arc origin. The Sc and Zr contents of continental rocks (mainly granitic and gneissose rocks) are higher than those of island arc-type volcanic rocks (Miyashiro and Kushiro, 1977). As Sc and Zr are more abundant in the Onnagawa Formation than in the Funakawa Formation, the terrigenous components of the Onnagawa Formation are considered to be derived mostly from the Asian continent, while those of the Funakawa Formation would have originated from the Japanese Island. This

speculation is supported by the $Rb-Al_2O_3$ relationships (Fig. 9).

The clay mineralogy also supports this interpretation. The dominant clay minerals in the Nishikurosawa and Onnagawa Formations are smectite and illite, while the Funakawa Formation is characterized by chlorite and smectite. The XRD patterns (peak width of illite) indicate that illite in the Nishikurosawa is not diagenetic component (Kubler, 1968).

Mineralogical studies on Quaternary sediments of the Japan Sea (Liu, 1985; Inoue and Naruse, 1990) indicate that illite is dominant in the terrigenous component derived from the continent. This argument suggests that the K/Ti ratio of sedimentary rocks should reflect the proportion of terrigenous input in the sediments. Therefore, the high K/Ti ratio for the periods ca 10.6–9.0 and 8.0–7.3 Ma (Onnagawa stage) (Fig. 10) may imply that considerable amounts of illite were input into the system from the Asian continent as eolian dust.

4.2. Paleo-oceanic redox conditions

Generally, the Mo, V, Co, Ni, Cu, Zn, and U contents of marine sediments reflect the redox conditions of deep seawater (Dean et al., 1997). Mo is particularly important as a paleoredox indicator as it is the most diagnostic of all of these redox elements (Jacobs et al., 1987; Emerson and Huested, 1991).

Fig. 11 shows the temporal variations in Mo/Al, Ni/Al and TOC. Mo/Al and Ni/Al increased rapidly at the Nishikurosawa/Onnagawa boundary, then decreased from the Onnagawa/Funakawa boundary. These data, particularly the Mo/Al ratio, suggest that the bottom water environment during the Onnagawa stage was reducing, with the most reductive periods being 12.7–11.7, 10.6–9 and 8.3–7.0 Ma.

The Ce anomaly is not positively correlate with Mo/Al or Ni/Al ratios. Probably, paleo-redox state recorded by Ce anomaly of sedimentary rocks studied were masked by terrigeneous components, hydrothermal effect and diagenetic process (e.g. Murray et al., 1991).

4.3. Biogenic productivity

It is generally accepted that the abundance of Si, P, and Ba in sedimentary rocks reflects the sea-surface

Table 4
Rare earth elements contents of sedimentary rocks studied

	Daizima-sawa area													Onnagawa-sawa area				
Sample No.	NK-01	NK-02	NK-03	NK-04	NK-05	NK-06	NK-07	NK-08	NK-09	NK-10	NK-11	NK-12	NK-13	OG-01	OG-02	OG-03	OG-04	OG-05
Lithology	Sh	Sh	sh	sh	sh	sh	sh	sh	sh	sh	sh	sh	sh	h. sh	h. sh	h. sh	h. sh	h. sh
Color	dk. gn.	dk. gn.	dk. gn.	dk. gn.	dk. gn.	dk. gn.	dk. gn.	dk. gn.	dk. gn.	dk. gn.	dk. gn.	dk. gn.	dk. gn.	dk. and lgt. gr.	dk. and lgt. gr.	Dk. And lgt. Gr.	dk. and lgt. gr.	dk. and lgt. gr.
La (ppm)	16.9	18.3	16.4	16.3	19.3	16.9	10.5	12.7	22.9	16.3	17.9	17.3	17.4	3.6	8.4	3.7	4.1	5.7
Ce	43.1	46.2	45.3	44.7	50.5	41.4	27.6	31.8	49.3	36.9	40.1	39.3	39.9	7.0	20.6	9.3	16.9	19.5
Pr	4.6	5.0	4.6	4.5	5.1	4.3	3.3	4.0	5.9	4.6	4.8	4.5	4.5	0.7	1.9	0.9	1.3	1.6
Nd	20.1	21.4	20.2	19.4	21.8	17.5	14.5	17.4	25.9	20.0	20.6	18.6	19.1	2.5	7.3	3.8	5.1	6.8
Sm	4.47	4.79	4.71	4.51	5.04	4.04	3.54	4.24	6.03	4.76	4.80	4.12	4.19	0.51	1.62	0.80	1.22	1.66
Eu	1.21	1.31	1.15	1.17	1.36	1.12	1.06	1.28	1.65	1.38	1.36	1.13	1.16	0.15	0.37	0.21	0.31	0.43
Gd	4.44	4.87	4.43	4.39	5.15	4.13	4.44	5.32	7.45	4.72	4.73	3.95	4.10	0.53	1.46	0.73	1.09	1.61
Tb	0.89	0.95	0.85	0.83	0.99	0.70	0.59	0.79	1.20	0.92	0.83	0.70	0.76	0.08	0.28	0.13	0.18	0.30
Dy	4.84	5.22	4.61	4.61	5.18	3.60	3.25	4.31	6.59	4.82	4.27	3.78	3.84	0.52	1.49	0.73	0.98	1.56
Ho	0.98	1.02	0.88	0.88	0.93	0.65	0.59	0.77	1.32	0.91	0.78	0.77	0.76	0.11	0.35	0.17	0.19	0.35
Er	2.95	3.00	2.55	2.63	2.83	2.01	1.81	2.35	3.88	2.60	2.15	2.22	2.24	0.35	1.02	0.48	0.50	1.02
Tm	0.43	0.45	0.40	0.38	0.45	0.31	0.28	0.36	0.66	0.43	0.31	0.36	0.34	0.06	0.18	0.08	0.09	0.16
Yb	2.77	2.83	2.37	2.44	2.64	2.03	1.69	2.21	3.93	2.56	1.87	2.22	2.31	0.41	1.36	0.59	0.53	1.12
Lu	0.42	0.43	0.35	0.36	0.39	0.29	0.25	0.32	0.58	0.36	0.28	0.33	0.35	0.08	0.22	0.09	0.08	0.18
Total REEs	108.1	115.7	108.8	107.2	121.6	99.0	73.5	87.8	137.4	101.2	104.8	99.2	101.0	16.5	46.6	21.7	32.6	42.1
Ce/Ce*	1.17	1.16	1.24	1.25	1.22	1.18	1.12	1.08	1.00	1.03	1.04	1.08	1.08	1.06	1.26	1.26	1.84	1.56
Eu/Eu*	1.27	1.27	1.18	1.23	1.25	1.28	1.24	1.24	1.14	1.37	1.34	1.31	1.31	1.31	1.13	1.13	1.25	1.23
La/Yb	0.48	0.51	0.54	0.53	0.57	0.65	0.49	0.45	0.46	0.50	0.75	0.61	0.59	0.69	0.49	0.49	0.62	0.40

Abbreviations are the same as those in Table 2. No entry below detection limit.

|																Nomura area			
OG-06 h. sh dk. and lgt. gr.	OG-07 h. sh dk. and lgt. gr.	OG-08 h. sh dk. and lgt. gr.	OG-09 h. sh dk. and lgt. gr.	OG-10 h. sh dk. and lgt. gr.	OG-11 h. sh dk. and lgt. gr.	OG-12 h. sh dk. and lgt. gr.	OG-13 h. sh dk. and lgt. gr.	OG-14 h. sh dk. and lgt. gr.	OG-15 h. sh dk. and lgt. gr.	OG-16 h. sh dk. and lgt. gr.	OG-17 h. sh dk. and lgt. gr.	OG-18 h. sh dk. and lgt. gr.	OG-19 h. sh dk. and lgt. gr.	OG-20 h. sh dk. and lgt. gr.	OG-21 h. sh dk. and lgt. gr.	FK-01 sh lgt. gr.	FK-02 sh lgt. gr.	FK-03 sh lgt. gr.	FK-04 sh lgt. gr.
11.2	10.7	5.6	3.9	9.8	14.6	3.1	9.3	8.1	21.6	5.3	5.6	10.8	13.1	12.3	8.3	17.6	17.3	20.5	19.4
40.0	42.8	14.6	12.7	30.1	40.9	3.5	21.2	20.5	59.5	26.5	17.8	32.6	33.7	33.2	23.5	43.3	42.0	51.8	46.7
3.0	3.1	1.1	1.4	2.8	4.7	0.7	2.1	2.0	6.1	3.2	1.5	2.7	2.6	2.5	1.7	4.4	4.3	5.4	4.7
12.2	12.6	3.9	5.9	12.3	19.3	3.3	7.5	8.0	24.8	16.1	6.0	10.5	9.5	9.3	6.1	17.8	16.7	21.6	19.2
2.64	2.57	0.70	1.62	3.39	4.96	0.66	1.64	1.77	5.08	4.86	1.39	2.18	1.81	1.82	1.13	3.76	3.65	4.78	4.06
0.59	0.64	0.21	0.41	0.82	1.16	0.19	0.33	0.40	1.16	1.17	0.32	0.51	0.40	0.43	0.30	0.91	0.79	1.07	0.91
2.73	2.68	0.84	1.47	2.98	4.33	0.92	1.51	1.85	4.87	4.20	1.45	2.12	1.93	2.13	1.32	3.69	3.42	4.66	4.21
0.42	0.43	0.13	0.23	0.51	0.72	0.14	0.24	0.31	0.87	0.76	0.24	0.36	0.30	0.35	0.20	0.69	0.64	0.87	0.72
2.07	2.43	0.69	1.24	2.47	3.67	0.78	1.36	1.70	4.56	3.78	1.28	1.89	1.73	1.86	1.17	3.66	3.36	4.62	3.90
0.43	0.44	0.15	0.23	0.45	0.69	0.15	0.29	0.38	0.87	0.63	0.26	0.38	0.35	0.36	0.24	0.71	0.68	0.91	0.77
1.20	1.33	0.55	0.71	1.40	1.83	0.57	0.99	1.14	2.51	1.86	0.85	1.14	1.14	1.05	0.82	2.16	2.12	2.66	2.36
0.20	0.21	0.10	0.12	0.22	0.31	0.08	0.19	0.19	0.37	0.27	0.14	0.19	0.19	0.19	0.15	0.35	0.35	0.46	0.39
1.39	1.41	0.79	0.81	1.45	1.94	0.54	1.32	1.26	2.37	1.96	1.07	1.23	1.37	1.20	0.99	2.29	2.06	2.87	2.38
0.19	0.21	0.14	0.12	0.21	0.29	0.09	0.23	0.19	0.30	0.25	0.16	0.21	0.19	0.18	0.14	0.36	0.35	0.41	0.37
78.3	81.5	29.6	30.8	68.9	99.4	14.7	48.1	47.8	135.0	70.8	38.0	66.8	68.3	66.9	46.1	101.6	97.7	122.5	110.1
1.69	1.83	1.43	1.34	1.38	1.23	0.55	1.20	1.24	1.28	1.41	1.51	1.49	1.40	1.44	1.49	1.20	1.20	1.21	1.18
1.04	1.13	1.27	1.25	1.21	1.17	1.11	1.00	1.04	1.10	1.22	1.06	1.11	1.01	1.01	1.11	1.15	1.05	1.06	1.04
0.63	0.60	0.56	0.38	0.53	0.59	0.45	0.55	0.50	0.72	0.21	0.41	0.69	0.75	0.81	0.69	0.60	0.66	0.56	0.64
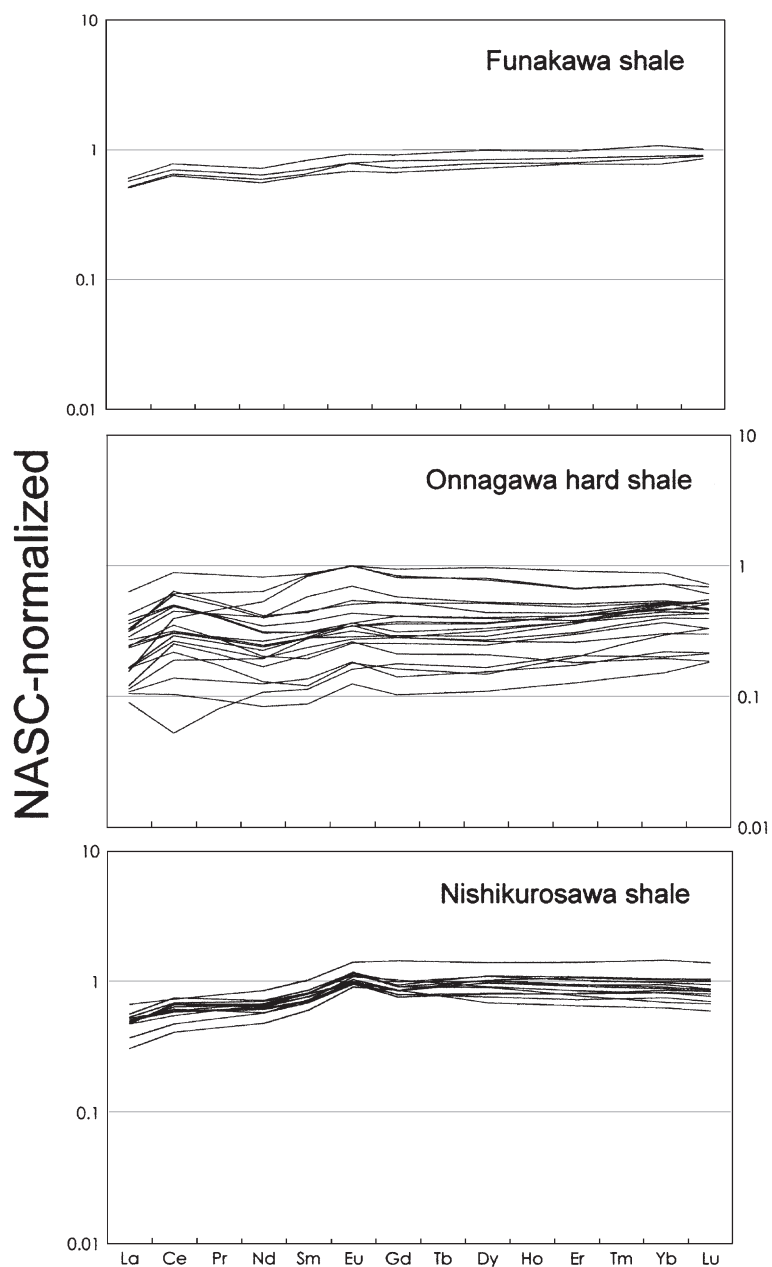
Fig. 6. The NASC-normalized REE pattern of sedimentary rocks studied.

biogenic productivity at the period of deposition (Si; Broecker and Peng, 1982; P; Arthur and Dean, 1998, Ba; Elderfield, 1990; Dean et al., 1997).

The abundances of these elements may also be related to hydrothermal activity and diagenesis. For example, SiO_2 and P are removed during diagenesis (e.g. Murray et al., 1991; Tada, 1991). The Si/Al, P/Al, and Ba/Al ratios does not solely reflect the sea-surface biogenic productivity. However, Fig. 12 indicates that the variations in P/Al, Si/Al and

Table 5
$^{87}Sr/^{86}Sr$ ratio, and Rb and Sr contents of sedimentary rocks studied

Sample No.	Lithology	Rb (ppm)	Sr (ppm)	$^{87}Sr/^{86}Sr$	$2\delta M$
FK-04	sh	79.72	17.44	0.708506 ±	12
FK-03	sh	79.56	18.07	0.707861 ±	13
FK-02	sh	93.89	14.41	0.708053 ±	16
FK-01	sh	52.43	107.38	0.707851 ±	14
OG-21	h. sh	38.78	35.86	0.711132 ±	24
OG-20	h. sh	31.85	33.04	0.709667 ±	27
OG-19	h. sh	31.62	26.68	0.711197 ±	15
OG-18	h. sh	24.02	21.22	0.710414 ±	21
OG-17	h. sh	29.39	27.56	0.710174 ±	19
OG-16	h. sh	26.39	15.24	0.714244 ±	19
OG-15	h. sh	30.99	21.30	0.711527 ±	18
OG-14	h. sh	31.91	25.98	0.710774 ±	13
OG-13	h. sh			n.a.	
OG-12	h. sh	16.42	18.80	0.709241 ±	25
OG-11	h. sh	39.14	38.13	0.711130 ±	13
OG-10	h. sh	37.95	29.92	0.710995 ±	14
OG-09	h. sh	32.72	22.14	0.713542 ±	26
OG-08	h. sh	30.33	18.81	0.712186 ±	21
OG-07	h. sh	39.06	37.20	0.710625 ±	13
OG-06	h. sh	37.73	42.32	0.709744 ±	17
OG-05	h. sh	18.26	28.33	0.709142 ±	9
OG-04	h. sh	16.95	27.33	0.709803 ±	17
OG-03	h. sh	23.08	22.11	0.710413 ±	21
OG-02	h. sh	40.95	38.25	0.711373 ±	21
OG-01	h. sh	23.46	30.33	0.709695 ±	12
NK-13	sh	48.57	238.29	0.706159 ±	23
NK-12	sh	47.66	210.90	0.706065 ±	22
NK-11	sh	52.94	266.45	0.706063 ±	22
NK-10	sh	33.73	235.72	n.a.	
NK-09	sh	30.92	364.64	0.706189 ±	17
NK-08	sh	34.03	308.90	0.706085 ±	16
NK-07	sh	36.70	295.44	0.706043 ±	25
NK-06	sh	36.96	273.91	0.705907 ±	26
NK-05	sh	48.62	202.27	0.705962 ±	15
NK-04	sh	40.34	138.24	0.706542 ±	19
NK-03	sh	37.74	124.58	0.706833 ±	21
NK-02	sh	37.17	175.00	0.706425 ±	22
NK-01	sh	35.74	142.07	0.706548 ±	17

Abbreviations are the same as those in Table 2. Data for granite, andesite and basalt is from Miyashiro and Kushiro (1977).

Ba/Al are roughly correlated with those in Mo/Al and Ni/Al. Therefore, the variations in these abundances may imply that a reducing deep-sea environment formed in association with a period of high biogenic productivity.

The TOC/N ratio between 8 and 9 indicates that TOC and N are marine planktonic origin (Redfield et al., 1963), as typical terrestrial organic matter has the TOC/N ratio greater than 20 (Hedges et al., 1986). Thus, the TOC and N contents of the Onnagawa shale are more influenced by terrestrial organic matter compared to the Nishikurosawa and Funakawa shales (Fig. 13).

4.4. Hydrothermal activity

Hydrothermal solution venting from mid-ocean ridges and back-arc basins is known to have a positive Eu anomaly (Michard et al., 1983; Klinkhammer et al., 1985; Michard, 1989; Shikazono, 1999). Therefore, the positive Eu anomaly of the sedimentary rocks is thought to be due at least in part to such a hydrothermal source. The following equation was used to estimate $Eu/Eu^*_{seawater}$ which represents the positive Eu anomaly of seawater at that time.

$$Eu/Eu^*_{rock} = n(Eu/Eu^*_{seawater}) + (1 - n) \times (Eu/Eu^*_{seawater})$$

where, n is the proportion of terrigenous component in the sediments, Eu/Eu^*_{rock} is the positive Eu anomaly of sedimentary rocks, and $Eu/Eu^*_{terrigenous}$ is the positive Eu anomaly of the terrigenous component. The value of n was calculated based on the average Zr content of the sedimentary rock and the Zr content of NASC (Zr = 160 ppm; Gromet et al., 1984) for 100% terrigenous sediment.

Fig. 14 shows the positive Eu anomaly of seawater at the Nishikurosawa, Onnagawa, and Funakawa stages. It seems likely from the Eu anomaly that intense hydrothermal activity occurred during the Nishikurosawa stage.

The intensity of hydrothermal activity decreased from the Nishikurosawa/Onnagawa boundary towards the Funakawa stage. However, it is noteworthy that hydrothermal activity also occurred at ca.12.6, 10.6, and 8.2 Ma. The hydrothermal signal at these ages is consistent with that for the Kuroko and vein-type mineralization ages. However, these are other explanation for the Eu anomaly.

It is also possible that feldspar with a positive Eu anomaly was entrained in the sedimentary rocks. However, there is no positive correlation between the Eu anomaly and the Al content, suggesting that
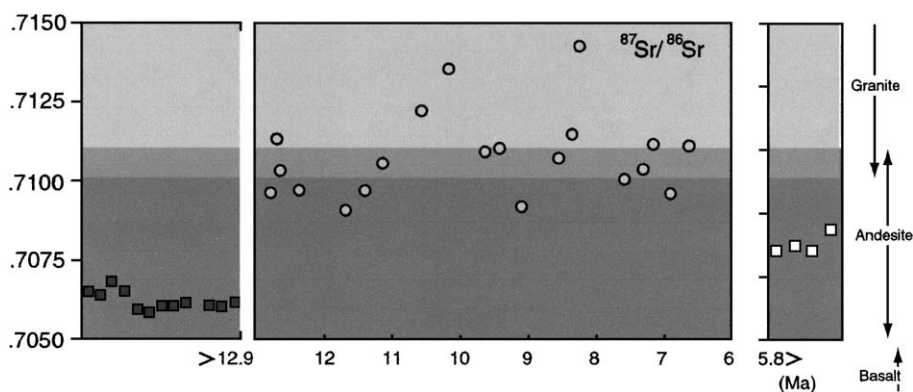
Fig. 7. Temporal variation in $^{87}Sr/^{86}Sr$ ratio of the sedimentary rocks studied. Solid squares: Nishikurosawa shale, open circles: Onnagawa hard shale, open squares: Funakawa shale.

feldspar does not contribute appreciably to the Eu anomaly.

The ratios of S/C ratios of the Onnagawa and Funakawa Formations are within the range typical for sedimentary rock, while that of the Nishikurosawa is comparatively high, suggestive of a supply of hydrothermal sulfur during the Nishikurosawa stage. The anomalously high Zn, and Ba of the Nishikurosawa sediments may reflect the presence of sphalerite and barite, again suggesting a hydrothermal contribution during the Nishikurosawa stage.

Table 6
Correlation coefficient (r) values, sedimentary rocks studied

	Al_2O_3		Al_2O_3		Al_2O_3
TiO_2	0.96	Sc	0.89	La	0.81
Fe_2O_3*	0.94	V	0.53	Ce	0.70
MnO	0.45	Cr	0.66	Nd	0.80
MgO	0.94	Co	0.49	Sm	0.77
CaO	0.82	Ni	− 0.04	Eu	0.82
Na_2O	0.91	Cu	− 0.42	Gd	0.81
K_2O	0.80	Zn	0.20	Tb	0.82
P_2O_5	0.00	Rb	0.68	Dy	0.83
		Sr	0.84	Ho	0.83
		Y	0.79	Er	0.84
		Zr	0.88	Tm	0.83
		Nb	0.94	Yb	0.81
		Mo	− 0.59	Lu	0.83
		Ba	− 0.31	Ce/Ce*	− 0.44
		Hf	0.96	Eu/Eu*	0.31
		Ta	0.90		
		Th	0.23		
		U	− 0.47		

4.5. Paleo-oceanic environment of the Japan Sea

The paleo-oceanic environmental change of the Japan Sea from the late Nishikurosawa to early Funakawa stage can be reconstructed based on the above geochemical data.

The Nishikurosawa stage (ca.16–12.9 Ma) is characterized by bimodal (basic and acidic) volcanism (Konda, 1974). The seawater depth at this time was shallow due to intense volcanic activity related to ascent of the asthenosphere. The depth estimated by Hasegawa et al. (1989) was between 30 and 200–1000 m. Terrigenous detritus was supplied from the island arc to shallow-depth seawater.

During the Nishikurosawa stage, intense hydrothermal activity is expected to have occurred, as deduced from the positive Eu anomaly of the sedimentary rocks. In particular, the positive Eu anomaly at the Nishikurosawa/Onnagawa boundary is very high (2.4), at a level similar to that of sediments below the hydrothermal pool of the Red Sea (Fish debris, Eu/Eu*=2.4–4.9; Oudin and Cocherie, 1988) (Fig. 14).

Foraminifera was dominant in the Nishikurosawa stage, while radiolarian was dominant in the Onnagawa stage. The microfossil data, together with the molluscan fossil data, indicate that the northern part of the Japan Sea during the Nishikurosawa stage was closed, and that a warm paleo-Kuroshio current entered through the Tsushima gateway. A cold paleo-Oyashiro current may have been introduced into the Japan Sea from the Pacific Ocean during the Onnagawa stage, as the southern part of the Japan
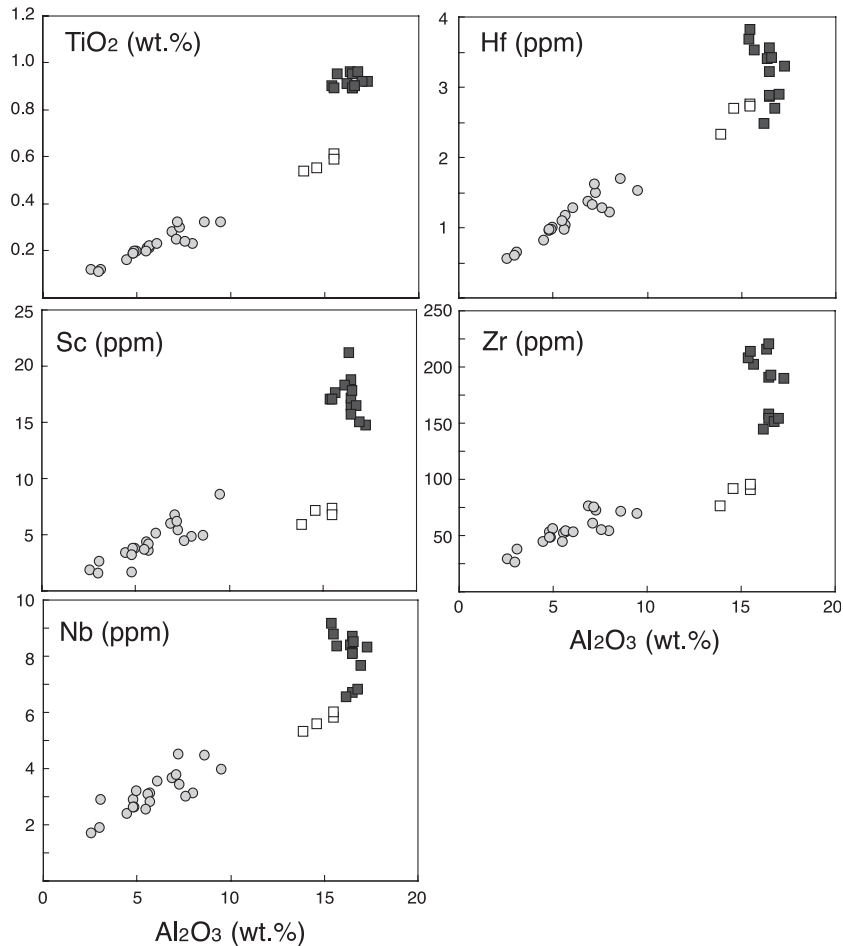
Fig. 8. Al_2O_3 content vs. selected element content. Symbols are the same as in Fig. 7.

Sea was closed probably due to the rapid clock-wise rotation of the Japanese Islands and the resultant opening of the Japan Sea basin (Chinzei, 1991).

Bimodal volcanism ceased during the Onnagawa stage and subsidence occurred during 13–8 Ma (Sato and Amano, 1991). According to Hasegawa et al. (1989), the depth of the Japan Sea became considerably deep (1000–2000 m) at the Nishikurosawa/Onnagawa boundary. Due to the subsidence, the island arc-derived component decreased in abundance and eolian dust (terrigenous component) from the Asian continent increased.

Mo/Al and Ni/Al, which are good indicators of the reduction state of bottom seawater, increased at the Nishikurosawa/Onnagawa boundary (ca.12.6 Ma), indicating that the deep sea changed rapidly from oxic condition to reducing condition at this boundary. This environmental change is considered to have been caused by stratification of the Japan Sea due to the introduction of the paleo-Oyashio current from the Pacific Ocean, having very low O_2 content (Kajiwara, 1983). However, the P/Al and Ba/Al ratios also increased at the Nishikurosawa/Onnagawa boundary, suggesting high biogenic productivity at the boundary. This high production probably also contributed to the reducing conditions of bottom seawater due to decomposition of sinking organic matter from the sea surface.

As already noted, the periods of 10.6–9 and 8.3–7.0 Ma are characterized by high TOC, Mo/Al, Ni/Al
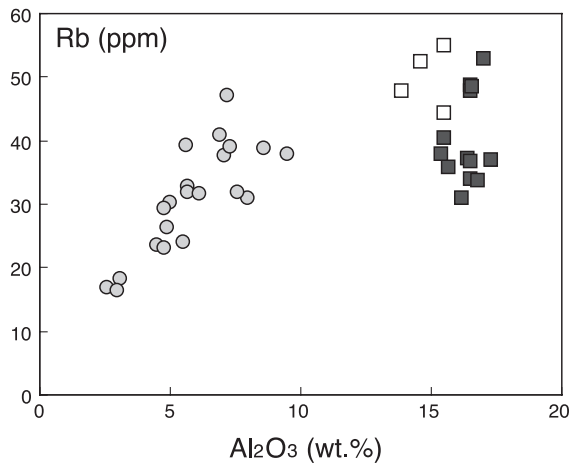
Fig. 9. Al_2O_3 vs. Rb. Symbols are same to those in Fig. 7.

and K/Ti ratios (Figs. 10 and 11). This stage also features a high proportion of terrigenous detritus, probably derived from the continent by wind. The continental eolian origin of the terrigenous component is likely because the $^{87}Sr/^{86}Sr$, K/Ti, and Rb/Ti ratios are high. Agitation of the surface seawater by the strong winds from the continent will also have maintained the high biogenic production rate at the surface.

As shown in Fig. 13, the close relationship between the TOC and terrigenous content suggests that the organic matter adsorbed readily onto the surface of

terrigenous particles, which might have resulted in aggregates with relatively high resistance to bacterial degradation (Waseda et al., 1995).

It is widely accepted that intensification of the Asian monsoon since the middle Miocene was related to the uplift and elevation of the Himalayan and Tibetan Plateau regions. In fact, a number of microfossils with activities related to the monsoon climate have been found in sediments of the Indian Sea (Prell and Kurtzbuck, 1992). Furthermore, the $\delta^{13}C$ record of the Pakistani Siwalik sediments shows that the monsoonal dynamics changed at about 8.5 Ma (Cerling et al., 1997, 1998).

Fig. 15 shows the $^{87}Sr/^{86}Sr$ ratio of the terrigenous component of the Onnagawa Formation, as estimated using the following equation.

$$^{87}Sr/^{86}Sr_{rock} = (n)^{87}Sr/^{86}Sr_{terrigenous}$$
$$+ (n-1)^{87}Sr/^{86}Sr_{seawater}$$

It is obvious from the figure that at 10.0 and 8.0 Ma, a terrigenous component with high $^{87}Sr/^{86}Sr$ ratio was mixed with the sediments. This suggests a high eolian input of material with a high $^{87}Sr/^{86}Sr$ ratio derived from the Asian continent.

In the Funakawa stage, the sediments included a higher detrital component compared to the Onnagawa sediments. The major elements, minor elements,
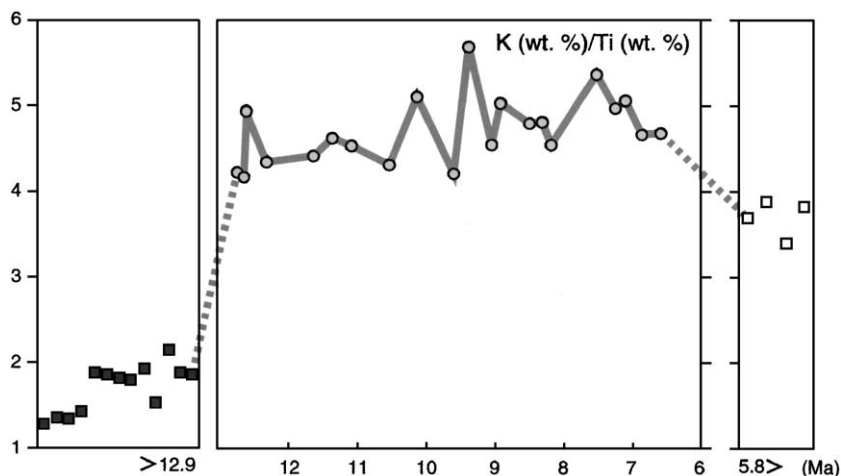
Fig. 10. Temporal variation in K/Ti ratio of the sedimentary rocks studied. Symbols are the same as in Fig. 7.
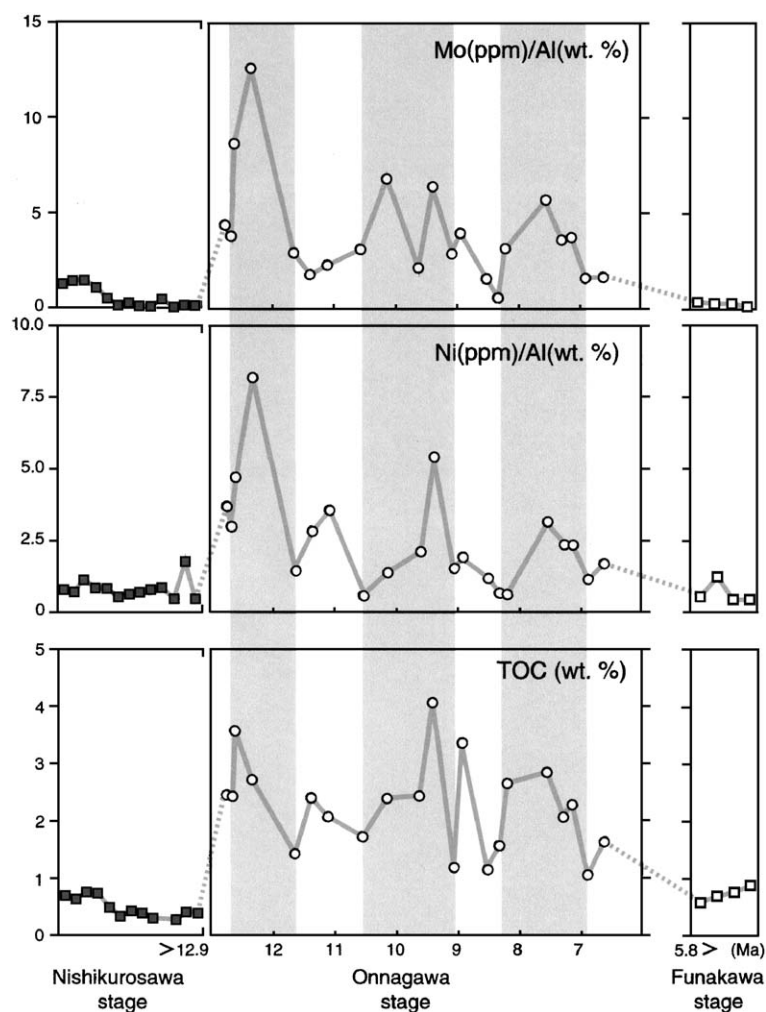
Fig. 11. Temporal variation in Mo/Al and Ni/Al ratios and TOC content of the sedimentary rocks studied. Symbols are the same as those in Fig. 7.

total REE and $^{87}Sr/^{86}Sr$ ratio of the Funakawa sedimentary rocks indicate that the terrigenous detritus component was supplied dominantly from an island arc environment. The increase in the smectite component of the Funakawa sedimentary rocks also supports this interpretation.

According to Sato and Amano (1991), the tectonic situation in the northeastern Japan arc was changed from subsidence to compressional at 8 Ma. This resulted in the uplift of the back-arc region of the Japan Sea shallower, giving rise to the increased supply of island arc materials.

5. Summary and conclusions

XRF and ICP-MS analytical studies of Miocene sedimentary rocks formed in the Japan Sea back-arc basin revealed that each formation (Nishikurosawa, Onnagawa and Funakawa) has different features; The biogenic SiO_2 content of the Onnagawa Formation is very high (av. 84.3 wt.%), compared to that of the Nishikurosawa (av. 57.69 wt.%) and Funakawa (av. 67.5 wt.%) Formations, while the Al_2O_3 content of the Nishikurosawa and Funakawa Formations is high compared to that of the Onna-
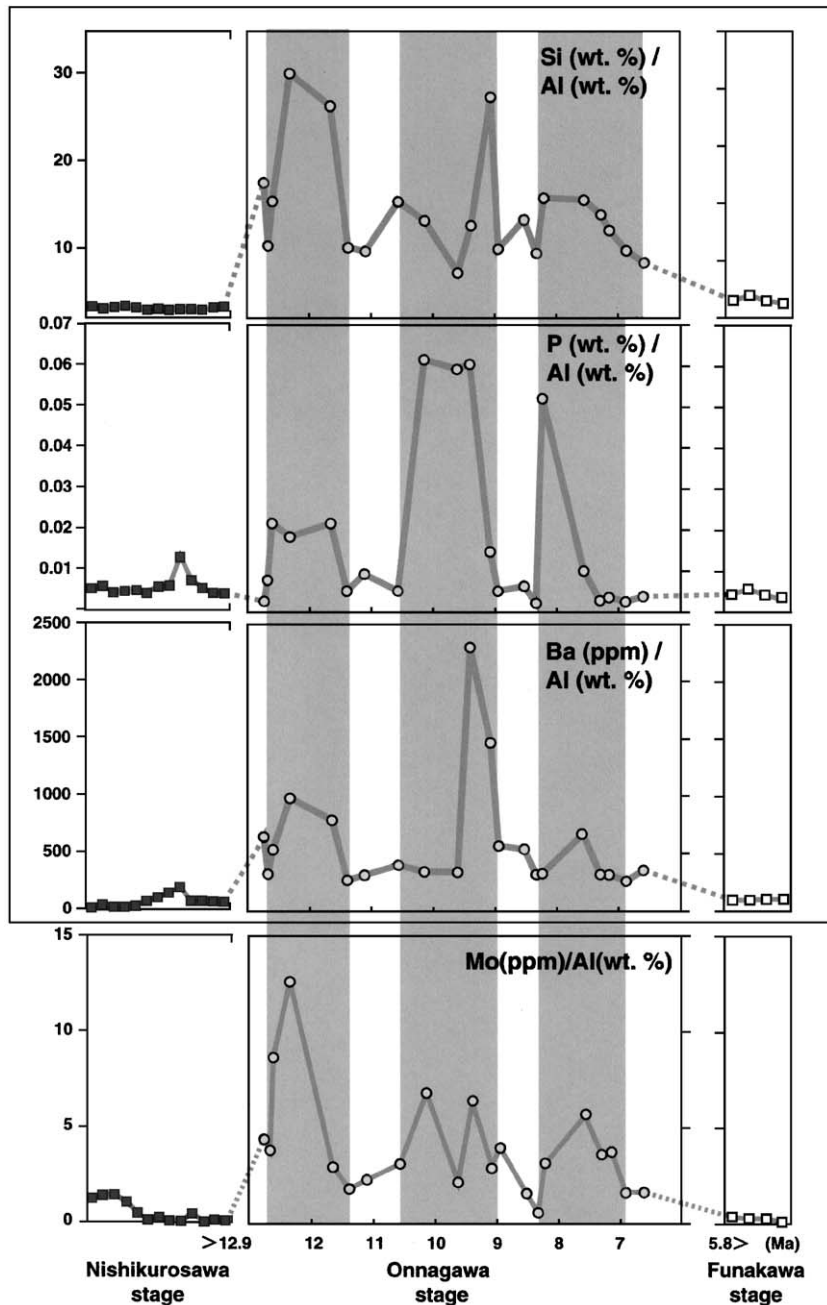
Fig. 12. Temporal variation in Si/Al, P/Al, Ba/Al and Mo/Al ratios of the sedimentary rocks studied. Symbols are the same as those in Fig. 7.

gawa Formation, indicating a small proportion of terrigenous component in the Onnagawa sediment, and higher proportion in the Nishikurosawa and Funakawa rocks.

The Ba/Al and P/Al of the Onnagawa Formation are higher than in the Nishikurosawa and Funakawa Formations, suggesting that the high biogenic productivity in the Onnagawa stage. Furthermore, the
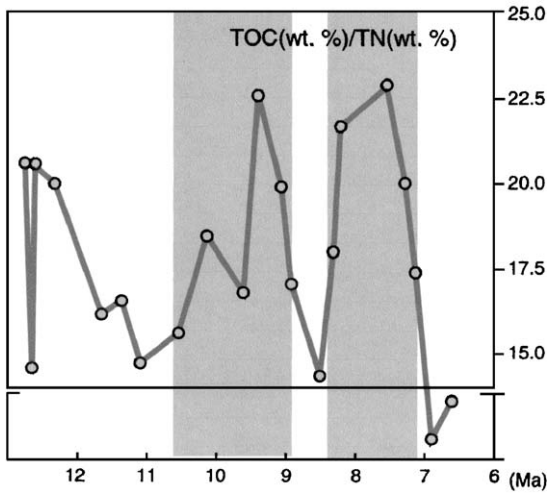
Fig. 13. Temporal variation in TOC/N ratio of the sedimentary rocks studied. Symbols are the same as those in Fig. 7.
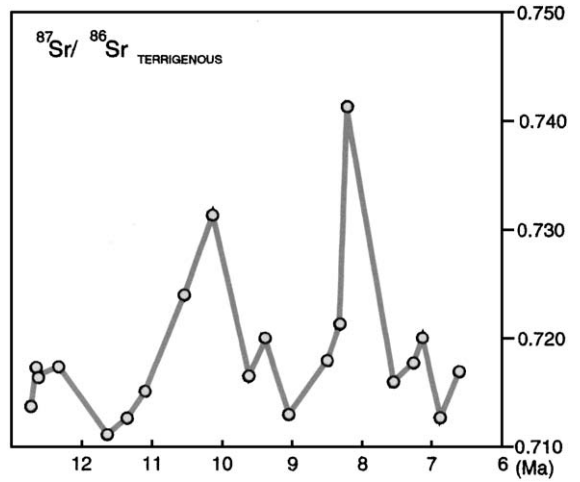
Fig. 15. ^{87}Sr/^{86}Sr ratio of terrigenous components in the sedimentary rocks studied.
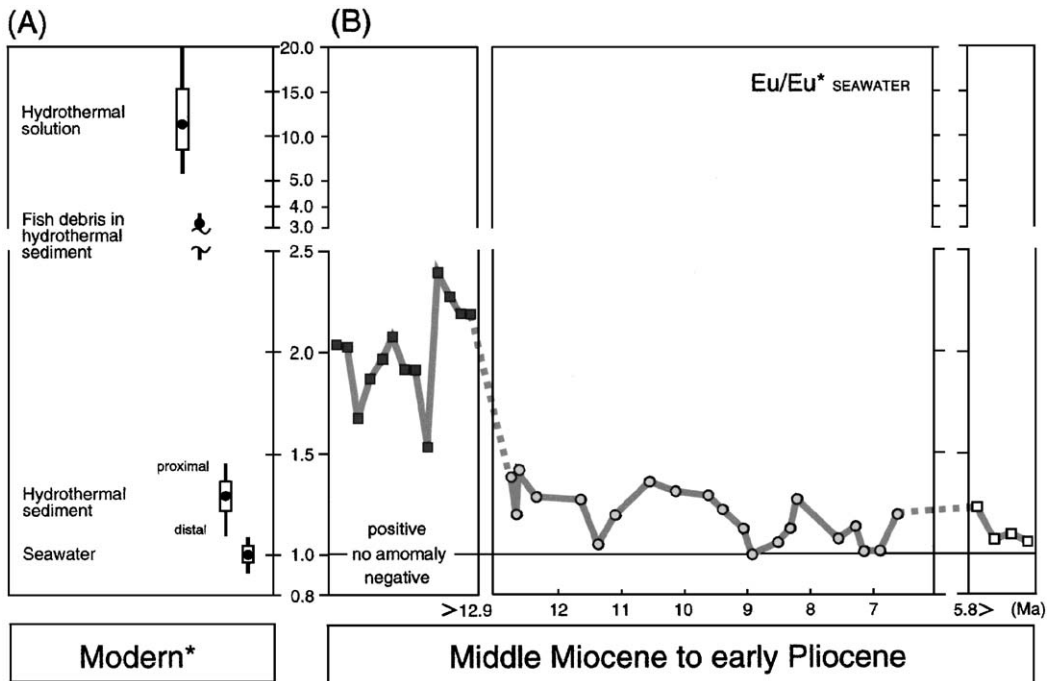
Fig. 14. Positive Eu anomaly of seawater at the Nishikurosawa, Onnagawa, and Funakawa stages. Modern data are from the Pacific Ocean, except fish debris in the hydrothermal sediment (Red Sea). Modern* is defined here as including Quarternally time. Data sources; Hydrothermal solution (Michard and Albarede, 1986); seawater (De Baar et al., 1985); fish debris in the Atlantic II deep (Oudin and Cocherie, 1988); hydrothermal sediment (Ruhlin and Owen, 1986).

Mo/Al, Ni/Al, Ba/Al and P/Al ratios are roughly correlated with each other, suggesting that the high biogenic productivity gave rise to a reducing paleooceanic deep-sea environment due to the consumption of dissolved O_2 by the decomposition of organic matter.

The $^{87}Sr/^{86}Sr$ ratio of the Onnagawa sedimentary rocks at 10.0 and 5.8 Ma are high (av. 0.71085), suggesting a high proportion of the terrigenous component derived from the Asian continent, probably as eolian dust, in the Onnagawa rocks.

The $^{87}Sr/^{86}Sr$ ratio also roughly correlates with the P/Al and Ba/Al ratios which indicate biogenic activity, and the Mo/Al, and Ni/Al ratios, which reflect reducing conditions of bottom seawater. This correlation suggests that the input of terrigenous detritus, high biogenic productivity in the surface seawater, and reducing conditions at the sea bottom are interrelated.

The uplift of the Himalayan–Tibetan region, which took place during 10–8 Ma, has been associated with the intensification of the Asian monsoon. The wind associated with this intensification is thought to be responsible for the increased influx of terrigenous eolian dust and caused the upwelling of deep seawater leading to the intense biogenic activity in the surface seawater. Settling of organic matter and terrigenous material to the bottom of the sea would then have promoted the formation of the reducing environment at the sea bottom.

The most important finding of this study is that the geochemical features of sedimentary rocks of the Japan Sea back arc basin reflect not only the input of terrigenous material, hydrothermal activity, biogenic productivity, and ocean circulation pattern, but also regional climate change caused by change in the tectonic situation of the Asian continent, probably related to the uplift of the Himalayan–Tibetan region.

References

Arthur, M.A., Dean, W.E., 1998. Organic-matter production and preservation and evolution of anoxia in the Holocene Black Sea. Paleoceanography 13, 395–411.

Bazhenova, O.K., Arefiev, O.A., 1990. Immature oils as the products of early catagenetic transformation of bacterial–algal organic matter. Org. Geochem. 16, 307–311.

Blow, W.H., 1969. Late middle Eocene to Recent planktonic foraminiferal biostratigraphy: International Conference on Planktonic Microfossils. 1st Proceeding 1, 199–421.

Broecker, W.S., Peng, T.H., 1982. Tracers in the Sea, Eldigiod Press, New York.

Cerling, T.E., Harris, J.M., MacFadden, B.J., Leakey, M.G., Quade, J., Eisenmann, V., Ehleriinger, J.R., 1997. Global vegetation change through the Miocene/Pliocene boundary. Nature 389, 153–158.

Cerling, T.E., Harris, J.M., MacFadden, B.J., Quade, J., Leakey, M.G., Eisenmann, V., Ehleriinger, J.R., 1998. Reply to Miocene/Pliocene shift one step or several by Kohler, M. et al., 1998. Nature 393, 127.

Chinzei, K., 1991. Late Cenozoic zoogeography of the Sea of Japan. Episodes 14, 231–234.

Dean, W.E., Gardner, J.B., Piper, D.Z., 1997. Inorganic geochemical indicators of glacial interglacial changes in productivity and anoxia on the California continental margin. Geochim. Cosmochim. Acta 61, 4507–4518.

De Baar, H.J.W., Bacon, M.P., Brewer, P.G., 1985. Rare earth elements in the Pacific and Atlantic Oceans. Geochim. Cosmochim. Acta 49, 1943–1959.

Elderfield, H., 1990. Traces of ocean paleoproductivity and paleochemistry: an introduction. Paleoceanography 5, 711–717.

Emerson, S., Huested, S.S., 1991. Ocean anoxia and the concentrations of molybdenum and vanadium in seawater. Mar. Chem. 34, 177–196.

Goldstein, S.I., Jacobsen, S.B., 1988. Rare earth elements in river waters. Earth Planet. Sci. Lett. 89, 35–47.

Gromet, L.P., Dymek, R.F., Haskin, L.A., Korotev, R.L., 1984. The "North American shale composite": its compilation, major and trace element characteristics. Geochim. Cosmochim. Acta 48, 2469–2482.

Hasegawa, S., Akimoto, K., Kitazato, H., Matoba, Y., 1989. Late Cenozoic paleobathymetric indices based on benthic foraminifers in Japan. Mem. Geol. Soc. Jpn. 32, 241–253 (in Japanese with English abstract).

Hedges, J.I., Clark, W.A., Quay, P.D., Suntos, U.D.M., 1986. Compositions and fluxes of particulate material in the Amazon river. Limnol. Ocean R. 31, 717–738.

Huzioka, K., Takayasu, T., 1965. Geological guidebook of the Oga Peninsula. Akita Univ. Min. Coll. Inst. Min. Geol., 1–42.

Iijima, A., 1994. Neogene, phosphatic and glauconitic sediments of the northwestern Pacific Rim: a comparison with the eastern Pacific Rim. In: Iijima, A., et al. (Eds.), Proc. 29th Int'l. Geol. Congr. Part C: siliceous, phosphatic and glauconitic sediments of the Tertiary and Mesozoic. VSP, Utrecht, pp. 5–16.

Imai, N., 1990. Multielement analysis of rocks with use of geo-

logical certified reference material by inductively coupled plasma mass spectrometry. Anal. Sci. 6, 389–395.

Ingle, J.C., 1981. The Monterey formation and related siliceous, phosphatic and glauconitic sediments of the Tertiary and Mesozoic. In: Iijima, A., et al. (Eds.), Proc. 29th Int'l. Geol. Congr. Part C: siliceous, phosphatic and glauconitic sediments of the Tertiary and Mesozoic. VSP, Utrecht, pp. 159–179.

Inoue, K., Naruse, T., 1990. Asian long-range eolian dust deposited on soils and paleosols along the Japan Sea coast. Quat. Res. 29, 209–222.

Irino, T.,1997. Quantification of Kosa (eolian dust) contribution to the sediments and reconstruction of its flux variation at ODP site 1797, the Japan Sea during the last 200 ky. Doctoral thesis, Univ. Tokyo.

Ivanov, V.V., Shcherban, O.V., 1983. Mineral matrix influence on the dynamics and products of organic matter catagenetic transformation. Org. Geochem. 4, 185–194.

Jacobs, L., Emerson, S., Huested, S.S., 1987. Trace element chemistry in the Carioca Trench. Deep-Sea Res. 34, 965–981.

Kajiwara, Y., 1983. Biostratigraphic evidence for delimiting the possible duration of Kuroko metallogenetic epoch. Min. Geol. Spec. Issue 11, 305–309.

Klinkhammer, G., Rona, P., Greaves, M., Elderfield, H., 1985. Hydrothermal manganese plumes in the Mid-Atlantic Ridge rift valley. Nature 314, 727–731.

Koizumi, I., Matoba, Y., 1991. On the top of the Nishikurosawa stage. Geol. Soc. Jpn., Mem. 32, 187–195 (in Japanese with English abstract).

Konda, T., 1974. Bimodal volcanism in northeast Japan arc. J. Geol. Soc. Jpn. 80, 207–216.

Kubler, B., 1968. Évaluation quantitative du métamorphisme par la cristallinite de líllite. Bull. Cent. Rech. Pau 2, 385–397.

Liu, T., 1985. Loess and the environment. Paleogeogr. Paleoclimatology Paleoecol., vol. 50. China Ocean Press, Beijing, pp. 241–271. 251 pp.

Michard, A., 1989. Rare earth element systematics in hydrothermal fluids. Geochim. Cosmochim. Acta 53, 745–750.

Michard, A., Albarede, F., 1986. The REE content of some hydrothermal fluids. Chem. Geol. 55, 51–60.

Michard, A., Albarede, F., Michard, G., Minster, J.F., Charlou, J.L., 1983. Rare-earth elements and uranium in high temperature solutions from East Pacific Rise hydrothermal vent field. Nature 303, 795–797.

Miyashiro, A., Kushiro, I., 1977. Petrology III. Kyoritsu, Tokyo. In Japanese.

Murray, R.E., Ten Brink, M.R.B., Brumsack, H.J., Gerlach, D.C., Russ III, G.P., 1991. Rare earth elements in Japan Sea sediments and diagenetic behavior of Ce/Ce*. Geochim. Cosmochim. Acta 55, 2453–2466.

Oudin, E., Cocherie, A., 1988. Fish debris record the hydrothermal activity in the Atlantic II Deep sediments (Red Sea). Geochim. Cosmochim. Acta 52, 177–184.

Prell, W.L., Kurtzbuck, J.E., 1992. Sensitivity of the Indian monsoon to forcing parameters and implications for its evolution. Nature 360, 647–652.

Redfield, A.C., Ketchum, B.H., Richards, F.A., 1963. The influence of organisms on the composition of seawater. In: Hill, M.H. (Ed.), The Sea. Wiley, New York, pp. 26–77.

Ruhlin, D.E., Owen, R.M., 1986. The rare earth element geochemistry of hydrothermal sediments from the East Pacific Rise: examination of a seawater scavenging mechanism. Geochim. Cosmochim. Acta 50 (3), 393–400.

Sato, H., Amano, K., 1991. Relationship between tectonics, volcanism, sedimentation and basin development, Late Cenozoic, central part of Northern Honshu, Japan. Sediment. Geol. 74, 323–343.

Shikazono, N., 1988. Chemistry of Kuroko Deposits. Syokabo, Tokyo. In Japanese.

Shikazono, N., 1999. Rare earth element geochemistry of Kuroko ores and hydrothermally altered rocks: implications for evolution of submarine hydrothermal system at back arc basin. Resour. Geol. Spec. (20), 23–30.

Tada, R., 1991. Origin of rhythmical bedding in middle Miocene siliceous rocks of the Onnagawa Formation, northern Japan. J. Sediment. Petrol. 61, 1123–1145.

Taguchi, K., 1961. Stratigraphical studies of the Neogene Tertiary in the southern part of the Oguni River, Mogami-gun, Yamagata Prefecture. J. Geol. Soc. Jpn. 67, 157–170 (in Japanese with English abstract).

Taylor, S.R., McLennan, S.M., 1985. The Continental Crust: its composition and evolution. Blackwell, Oxford, England.

Utada, M., Ishikawa, Y., Takahashi, T., Hashiguchi, H., 1982. The distribution of alteration zones in the western area (Hanaoka-Matsumine-Shakanai mineralization area) of the Hokuroku district, northeast Japan. Min. Geol. Spec. Issue 11, 125–138.

Waseda, A., Tsuji, R., Kajiwara, Y., Nishido, H., 1995. Organic facies and depositional environment of the Opnnagawa Formation—comparison with the Montery Formation. J. Jpn. Assoc. Pet. Tech. 60, 49–61.

Watanabe, Y., Yamamoto, M., Imai, N., 1994. Preliminary assessment for hydrocarbon potential by sedimentary basin modeling: case study on the sedimentary environment of the Neogene Onnagawa source rock facies. Bull. Geol. Surv. Jpn. 45, 509–525.

Yamamoto, M., Watanabe, Y., 1994. Biomarker geochemistry and paleooceanography of Miocene Onnagawa diatomaceous sediments, northern Honshu, Japan. Proc. 28th. Int'l. Geol. Congr. Part C. VSP, Utrecht, pp. 53–74.